Journal of Experimental Botany, Vol. 58, No. 7, pp. 1677–1693, 2007
doi:10.1093/jxb/erm018 Advance Access publication 12 April, 2007
This paper is available online free of all access charges (see http://jxb.oxfordjournals.org/open_access.html for further details)

Journal of Experimental Botany
www.jxb.oxfordjournals.org

RESEARCH PAPER

Arabidopsis peroxin 16 trafficks through the ER and an intermediate compartment to pre-existing peroxisomes via overlapping molecular targeting signals

Sheetal K. Karnik and Richard N. Trelease*

Arizona State University, School of Life Sciences, PO Box 874501, Tempe, AZ 85287-4501, USA

Received 15 September 2006; Revised 8 January 2007; Accepted 22 January 2007

Abstract

Previously it has been shown that the endogenous *Arabidopsis* peroxin, AtPEX16, coexisted at steady state in membranes of the endoplasmic reticulum (ER) and peroxisomes. Herein, an ER-to-peroxisome trafficking pathway and the requisite molecular targeting signals for *myc*AtPEX16 transiently expressed in *Arabidopsis* and tobacco BY-2 suspension cells are described. Immunofluorescent *myc*AtPEX16 was observed initially in the cytosol (<2 h) and subsequently (2–4 h) in perinuclear/reticular ER and non-Golgi/non-peroxisome structures termed the ER-peroxisome intermediate compartment. After 4 h, all catalase- and ascorbate peroxidase-containing peroxisomes also possessed *myc*AtPEX16, indicative of *myc*AtPEX16 sorting to pre-existing peroxisomes. Incubations of bombarded cells at 15 °C, or in brefeldin A at 25 °C, resulted in accumulations of *myc*AtPEX16 within the ER. Following re-equilibration of cold-treated cells at 25 °C, or removal of brefeldin A, *myc*AtPEX16 was observed mainly in the ER-peroxisome intermediate compartment, and later within all of the peroxisomes in both species. Two internal membrane helices and the intervening sequence including the amino acid residues -VRS- were found necessary and sufficient for targeting AtPEX16 first to the ER and then to peroxisomes. Individual targeting signals for these organelles were indistinguishable, indicative of overlapping signal(s). In summary, the trafficking study of AtPEX16 revealed a dynamic link between the ER and pre-existing peroxisomes, which provided novel data in support of an upgraded semi-autonomous peroxisome model portraying participation of the ER in the sorting of certain peroxisome membrane proteins, such as AtPEX16, through an intermediate compartment to pre-existing plant peroxisomes.

Key words: *Arabidopsis thaliana* suspension cells, ascorbate peroxidase, brefeldin A, immunofluorescence microscopy, inter-organellar targeting signals, peroxins, peroxisome membrane protein, reticular endoplasmic reticulum, tobacco BY-2 cells, transient protein expression.

Introduction

An important feature of peroxisomes is their lack of DNA and protein synthesizing machinery, which dictate post-translational acquisitions from the cytosol of virtually all of their nuclear-encoded matrix and peroxisome membrane proteins (PMPs) (Sparkes and Baker, 2002; Erdmann and Schliebs, 2005). Peroxin (*PEX*) genes code for peroxins (PEX), which are proteins that mediate multiple aspects of peroxisome biogenesis such as ontogeny, maturation (differentiation), and multiplication (duplication and induced proliferation). A consecutive numbering system was created to identify and compare *PEX* genes and their corresponding peroxin homologues (Distel *et al*., 1996). To date, 23 plant peroxins have been identified. One of these homologues, peroxin 16, has been identified in *Arabidopsis* (AtPEX16) (Lin *et al*., 1999) and in only two other species, namely humans (HsPEX16) (Kim *et al*., 2006) and the yeast *Yarrowia lipolytica* (YlPEX16) (Titorenko and Rachubinski, 1998).

Lin *et al*. (1999) first reported that the *Arabidopsis SSE1* (*shrunken seed*) gene coded for the putative plant peroxin 16 homologue—AtPEX16. More recently, Lin *et al*. (2004) discovered that normal peroxisomes were not present in *sse1* mutant embryos and that a GFP chimeric

* To whom correspondence should be addressed. E-mail: d.trelease@asu.edu

protein (GFP–AtPEX16) complemented the mutation resulting in normal seed development. Furthermore, in plants stably transformed with GFP–AtPEX16, autofluorescent peroxisomes in root hairs and embryos re-affirmed that AtPEX16/sse1, like YlPEX16 and HsPEX16, was a peroxin homologue. Subsequently it was found that this membrane protein coexisted at steady state in the endoplasmic reticulum (ER) and peroxisomes of *Arabidopsis* suspension culture cells (Karnik and Trelease, 2005). The present results and those of Lin *et al*. (1999) are consistent with postulates that PEX16 homologues, including AtPEX16, are 'early peroxins' that function in ER-related biogenesis of peroxisomes (Titorenko and Rachubinski, 2001*a*; Eckert and Erdmann, 2003; Baker and Sparkes, 2005; Brocard *et al*., 2005; Kim *et al*., 2006).

Over the past few years, the long-standing 'autonomous peroxisome growth and division' model (Lazarow and Fujiki, 1985) that specifically disclaims any involvement of the ER (Purdue and Lazarow, 2001) has lost consensus support. During this same period, the biogenetic relationship between the ER and peroxisomes in diverse organisms has become almost generally accepted (Eckert and Erdmann, 2003; Lazarow, 2003; Baker and Sparkes, 2005; Kunau, 2005; Titorenko and Mullen, 2006; Trelease and Lingard, 2006; Van der Zand *et al*., 2006). Compelling evidence for ER involvement has come from diverse studies employing different approaches with yeasts, mammals, and plants. In the case of yeasts and mammals, an important overall distinction now is that the ER is regarded as the site at which new peroxisomes are directly formed as incipient pre-peroxisomal vesicles or membrane fragments (Geuze *et al*., 2003; Hoepfner *et al*., 2005; Kragt *et al*., 2005; Tam *et al*., 2005; Haan *et al*., 2006; Kim *et al*., 2006; Titorenko and Mullen, 2006). Thereafter, the detached 'pre-peroxisomes' variously acquire additional matrix and membrane proteins from the cytosol, and then they mature into functional organelles (Titorenko and Mullen, 2006; Trelease and Lingard, 2006; van der Zand *et al*., 2006). An important point in the case of plant peroxisomes is that no evidence exists for the formation (ontogeny) of any type of plant peroxisome directly from any segment of the ER (Mullen *et al*., 2001*a*; Baker and Graham, 2002; Trelease and Lingard, 2006). Instead, the plant ER is envisaged as the platform from which membrane components (peroxisome proteins and lipids) are derived and delivered in some sort of membrane carrier(s) to different classes of pre-existing plant peroxisomes, which undergo 'maturation' and divide to produce new daughter peroxisomes (Lingard and Trelease, 2006). All of these features have been incorporated recently into a composite working model called the 'semi-autonomous peroxisome maturation and replication' model (Mullen and Trelease, 2006). Within the context of this recent scheme, we sought in the current study to elucidate the dynamic intracellular relationship of AtPEX16 between the ER and peroxisomes in two different plant cells.

The preponderance of endogenous AtPEX16 throughout the 'general' ER and its coexistence within the peroxisomes in *Arabidopisis* suspension cells (Karnik and Trelease, 2005) provided a unique opportunity to dissect and elucidate the overall trafficking pathway of this PMP. Transiently expressed *myc*-epitope-tagged AtPEX16 was traced via immunofluorescence microscopy from its first appearance in the cytosol ultimately to peroxisomes in both *Arabidopsis* and tobacco BY-2 cells. These two cells types were included in the study to assess the commonality of trafficking pathways within different plant species. Observations were made during normal time-courses and compared with observations made during time-courses in which experimental treatments were imposed to impair trafficking through the ER, i.e. low temperature and brefeldin A (BFA) treatments. These experiments revealed the existence of a perceived, but not previously described, compartment in these cells, generally referred to as an 'ER-peroxisome intermediate compartment' (ERPIC) (Titorenko and Mullen, 2006). In addition, site-directed mutagenesis of AtPEX16 was employed to elucidate putative necessary and/or sufficient targeting signals within the pathway. Virtually the same results from all of these experiments with *Arabidopsis* and BY-2 cells collectively validated and revealed new data relative to PMP trafficking in recent model(s) portraying semi-autonomous peroxisome maturation and replication during plant peroxisome biogenesis.

Materials and methods

Suspension cell cultures, microprojectile bombardment, and (immuno)fluorescence microscopy

Suspension cell cultures of *Arabidopsis thaliana* var. Landsberg *erecta* and *Nicotiana tabacum* L. cv. Bright Yellow (BY-2) were grown and maintained as described previously by Lisenbee *et al*. (2003*a*) and Lee *et al*. (1997), respectively. Cells were harvested 4-d post-subculture for transient transformations accomplished via microprojectile biolistic bombardments, which were done according to procedures described in Karnik and Trelease (2005) and Flynn *et al*. (2005). Cells were spread on filter paper pre-moistened with transformation buffer, bombarded, and were allowed to transiently express gene products for varied times in the dark between 2 h and 23 h depending upon the experiment. Cells were fixed in 4% formaldehyde (prepared from paraformaldehyde) for 1 h and then processed using the standard tube procedure for immunofluorescence microscopy as described previously (Karnik and Trelease, 2005).

Antibody concentrations, room temperature incubation times, and sources were as follows: mouse anti-*c myc* monoclonal antibodies (1:500, 1 h; purified 9E10; Covance Research Products, Inc. Berkley, CA, USA), rabbit anti-cottonseed catalase IgGs (1:500, 1 h) (Kunce *et al*., 1988), rabbit anti-castor calnexin antiserum (1:500, 1 h; provided by Sean Coughlan (Coughlan *et al*., 1997), rabbit anti-cucumber peroxisomal ascorbate peroxidase (APX) IgGs (1:500, 4 h; Corpas *et al*., 1994), rabbit anti-*Arabidopsis* AtSec21 antiserum

(1:500, 1 h; provided by David Robinson (Movafeghi *et al*., 1999), *Arabidopsis* Sec23 antiserum (Pimpl *et al*., 2000), rabbit anti-mouse Sec23 (Hobman *et al*., 1998), goat anti-rabbit rhodamine (1:1000), goat anti-rabbit Cy2 (1:500, 1 h), goat anti-mouse Cy2 (1:500, 1 h), goat anti-rabbit Cy5 (1:500, 1 h), and goat anti-mouse Cy5 (1:500, 1 h). All of these fluorophore-conjugated secondary antibodies were purchased from Jackson ImmunoResearch Laboratories (Westgrove, PA, USA). Control experiments included omitting primary or secondary antibodies and/or substituting irrelevant antibodies or null serum for primary antibodies.

Fluorescence images were acquired using either a Zeiss Axiovert 100 epifluorescence microscope (Carl Zeiss, Thornwood, NY, USA) equipped with a CoolSnap ES CCD camera (Roper Scientific, Tucson, AZ, USA) or with a Leica DM RBE microscope equipped with Leica TCS NT scanning head (Leica, Heidelberg, Germany). The images were deconvolved using MetaMorph software (Universal Imaging Corp., Downingtown, PA, USA), and were assembled and adjusted for brightness, contrast, and pseudo-coloration using Adobe Photoshop 7.0 (Adobe Photosystems, Mountain View, CA, USA).

Cold (15 °C) and BFA treatments of bombarded cells

Arabidopsis and BY-2 suspension cells harvested and washed free of culture media were plated on filter papers pre-moistened with transformation medium and biolistically bombarded with 10 μg of plasmid DNA as described above.

Plated cells used for cold-treatment experiments were allowed to equilibrate at room temperature (25 °C) in the dark for 15 min, and were then incubated at 15 °C in the dark for up to 5 h. Cells from some of these plates (15 °C, 5 h) were scraped from the filter paper and fixed for 1 h at room temperature in 4% (v/v) formaldehyde (no recovery period at 25 °C). Other plates (15 °C, 5 h) were transferred to 25 °C (in darkness) and held for 30 min, 1 h, 1.5 h, 2 h, or 6 h before being scraped from the plates and fixed in 4% (v/v) formaldehyde. All fixed cells were washed in phosphate-buffered saline (PBS), cell walls were perforated/digested with 0.1% (w/v) Pectolyase Y-23 (Seishin Pharmaceutical, Tokyo, Japan) plus 0.05% (w/v) Cellulase RS (Karlan Research Products, Santa Rosa, CA, USA) for *Arabidopsis* and 0.1% Pectolyase Y-23 for BY-2 cells at 30 °C for 2 h, and 0.1 ml portions of cells were permeabilized in 0.3% (v/v) Triton X-100 (Sigma-Aldrich) in PBS for 15 min. Cells were then incubated at room temperature for 1 h each in primary and fluorophore-conjugated secondary antibodies diluted in PBS.

For BFA experiments, *Arabidopsis* and BY-2 cells were biolistically bombarded with 10 μg of plasmid DNA, incubated on plates at room temperature in 100 μg ml^{-1} BFA in transformation buffer and processed for immunofluorescence microscopy as described by Mullen *et al*. (1999). In control experiments, medium plus an appropriate amount of DMSO (Fisher) were used for all steps through bombardment. For recovery experiments, cells biolistically bombarded with *myc*AtPEX16 in the presence of BFA were incubated for 5 h with BFA, scraped from filter papers, and washed twice in medium minus BFA, and then incubated for an additional 6 h in medium minus BFA. These cells were then fixed in formaldehyde and processed for immunofluorescence microscopy.

Construction of plasmids

Molecular biology reagents were purchased from New England Biolabs (Beverly, MA, USA), Promega (Madison, WI, USA), Fermentas (Hanover, MD, USA), or Takara Biomedicals (Otsu, Shiga, Japan). Standard recombinant DNA procedures were used, and whole-plasmid PCR-based mutagenesis reactions were carried out using 'Quick change' Site-Directed Mutagenesis Kit (Stratagene, La Jolla, CA, USA). Genetech Biosciences (Tempe, AZ, USA) synthesized the oligonucleotide primers and dye terminator DNA cycle sequencing was done at Arizona State University DNA Laboratory (Tempe, AZ, USA).

Karnik and Trelease (2005) described the plasmid construction of the pRTL2 plasmids with the *myc*AtPEX16 gene; these plasmids contained the 35S cauliflower mosaic virus promoter. pRTL2/GFPAtPEX16 was constructed as follows. Construction of pRTL2/GFP was described elsewhere (Lisenbee *et al*., 2003*b*). PCR amplification of the open reading frame (ORF) of AtPEX16 was done with a forward primer that introduced an *Nhe*I site (SK1, Table 1) and a reverse primer that introduced an *Xba*I site and a stop codon (SK2). The product was TA-cloned into pCR2.1, digested with *Nhe*I and *Xba*I and then ligated into *Xba*I-digested pRTL2/GFP vector to yield pRTL2/GFPAtPEX16. pRTL2/GFPmAtPEX16 was constructed by a single change at amino acid residue 206 within GFP that prohibits dimer formation (Zacharias *et al*., 2002; Lisenbee *et al*., 2003*b*). The A206K mutation was inserted into the ORF of GFP in the pRTL2/GFPAtPEX16 template. The PCR reaction included forward (SK3) and reverse (SK4) primers that introduced mutation directly in the pRTL2/GFPAtPEX16 template.

pRTL2/GFPmAtPEX16 (211–310) was generated in two steps. First a PCR reaction including a forward primer (SK5) and a reverse primer (SK6) amplified base pairs 633–930 from the ORF of AtPEX16 and introduced an in-frame *Nhe*I site at the 5′ end and an *Xba*I site at the 3′ end. The PCR product was TA cloned and then

Table 1. *Synthetic DNA primers used to create plasmid constructs in this study*

Primer	DNA sequence
SK1	5′-CATGCTAGCGAAGCTTATAAGCAATGGGTTTGGAG-3′
SK2	5′-CTGCTCTAGAACCTCACGATCCCGATATGTAAGTG-3′
SK3	5′-CCTGTCCACACAATCTAAGCTTTCGAAAGATCCC-3′
SK4	5′-GGGATCTTTCGAAAGCTTAGATTGTGTGGACAGG-3′
SK5	5′-CATGCTAGCGCAGTTATAGAGCCTCCAATG-3′
SK6	5′-GCTCTAGAACCTCACAGTTTTCGTCTCCTCAGCTC-3′
SK7	5′-GAAAAGGATGAGCTGGGAGGTGGAAAACTGATATGGGC-3′
SK8	5′-GCCCATATCAGTTTTCCACCTCCCAGCTCATCCTTTTC-3′
SK9	5′-CCAATGATCAAGGAGGGAGGTGGAACGATGTCCGAGC-3′
SK10	5′-GCTCGGACATCGTTCCACCTCCCTCCTTGATCATTGG-3′
SK11	5′-CGTTCTTTTCATCGGAGGTGGTGGAGTCCGATCTTG-3′
SK12	5′-CAAGATCGGACTCCACCACCTCCGATGAAAAGAACG-3′
SK13	5′-CATCGGAGGTGGTGGAGGTGGAGGATGGATTCCTTGGGC-3′
SK14	5′-GCCCAAGGAATCCATCCTCCACCTCCACCACCTCCGATG-3

*Nhe*I and *Xba*I digested. The digested product was then ligated into *Xba*I-digested pRTL2/GFPmAtPEX16. Whole-plasmid-PCR-based mutagenesis was then used to generate all the other pRTL2/GFPmAtPEX16 constructs from the pRTL2/GFPmAtPEX16 (211–310) template.

With the exceptions of pRTL2/*myc*AtPEX16RRR(306–308)ΔGGG, pRTL2/*myc*AtPEX16RRR(221–223)ΔGGG, pRTL2/*myc*AtPEX16RKY(258–260)ΔGGG, and pRTL2/*myc*AtPEX16RKYGVRS(258–264)Δ6G, all the other pRTL2/*myc*AtPEX16 mutants were carried out by deleting amino acids using whole-plasmid PCR-based mutagenesis with pRTL2/*myc*AtPEX16 as template DNA. To generate pRTL2/*myc*AtPEX16RRR(306–308)ΔGGG, a forward primer (SK7) and a reverse primer (SK8), which introduced nucleotide base substitutions coding for glycine residues in place of arginine residues (306–308), was used. pRTL2/*myc*AtPEX16RRR (221–223)ΔGGG was generated using a forward primer (SK9) and a reverse primer (SK10), which introduced nucleotide base substitutions coding for glycine residues in place of arginine residues (221–223). pRTL2/*myc*AtPEX16RKY(258–260)ΔGGG was generated using a forward primer (SK11) and a reverse primer (SK12), which introduced nucleotide base substitutions coding for glycine residues in place of the arginine–lysine–tyrosine coding sequence. To generate pRTL2/*myc*AtPEX16RKYGVRS(258–264) Δ7G, pRTL2/*myc*AtPEX16RKY(258–260)ΔGGG was used as template DNA and a forward primer (SK13) and a reverse primer (SK14) were used, which introduced nucleotide base substitutions coding for glycine residues in place of the valine–arginine–serine coding sequence.

The plasmid construct coding for GmMan1::(GFP) was provided by Andreas Nebenführ (University of Tennessee, Knoxville, TN, USA) and Andrew Staehelin (University of Colorado, Boulder, CO, USA). It lacked the catalytic domain of mannosidase and contained targeting sequences that confer specific sorting to Golgi bodies (Nebenführ *et al*., 1999).

Results

Trafficking of transiently expressed myc*AtPEX16 from the cytosol to pre-existing peroxisomes*

Figure 1 is a grouping of immunofluorescence images showing the subcellular localization(s) of transiently expressed *myc*AtPEX16 at varied time points post-biolistic bombardment in *Arabidopsis* and BY-2 suspension-cultured cells. At the earliest detectable stage of expression (1.5 h), *myc*AtPEX16 was observed throughout the non-organellar cytoplasm, characteristic of a diffuse cytosolic immunofluorescence signal (Fig. 1A, O), rather than within punctate catalase-containing peroxisomes (arrowheads) in the same transformed cells (Fig. 1B, P). *Arabidopsis* peroxisomes characteristically are less numerous and more pleomorphic than the smaller more spherical BY-2 peroxisomes (Lisenbee *et al*., 2003*a*; Lingard and Trelease, 2006). At a slightly later time (2 h), *myc*AtPEX16 in most of the transformed cells was observed within perinuclear and cytoplasmic reticular ER (Fig. 1C, Q). These *myc*AtPEX16 localizations were identified as ER through colocalizations with the ER markers anti-calnexin IgGs separately (Fig. 1D, R) and in merged images (Fig. 1E, S, yellow). The same colocalizations were observed with Concanavalin A-Alexa 594 as the ER marker probe (data not shown). Evidence that *myc*AtPEX16 in *Arabidopsis* and BY-2 cells sorted within 2 h to the ER rather than to peroxisomes is presented in Fig. 1F, H, T, V. Open arrowheads in Fig. 1F, T point to sites of *myc*AtPEX16 in representative portions of perinuclear and reticular cytoplasmic ER that do not colocalize with anti-catalase IgGs in peroxisomes (solid arrowheads) of the same transformed cells (separately in Fig. 1G, U, and merged in Fig. 1H, V).

Between 2.5 h and 3.5 h post-bombardments, *myc*AtPEX16 in the various transformed cells was observed within varied structures, ranging from mostly recognizable ER to mostly recognizable peroxisomes. Of particular interest, however, was that a substantial portion of the *myc*AtPEX16 in both plant cell types was observed also in punctate structures (solid arrowheads in Fig. 1I, W) that were distinct from catalase- and *myc*AtPEX16-containing peroxisomes in the same cells (arrows in Fig. 1I, J, W, X). This distinction is more clearly observed in the merged images of the whole cells and enlargements within the insets (Fig. 1K, Y). The enlarged views of these green, *myc*AtPex16-containing non-peroxisomal structures reveal a varied, rather non-distinctive morphology, which *per se* does not convey definitive identification of these structures.

Figure 1L–N, A-1–C-1 shows that *myc*AtPEX16 in transformed cells examined between 4–8 h post-bombardments had sorted exclusively to catalase-containing peroxisomes in the same transformed cells (clearly evident in merged images Fig. 1N, C-1. Red-coloured peroxisomes without *myc*AtPEX16 are observed in nearby non-transformed cells. Significantly, all of the peroxisomes in the transformed cells appeared yellow/orange indicative of all of the catalase-containing peroxisomes in transformed cells possessing *myc*AtPEX16, i.e. expressed *myc*AtPEX16 and endogenous catalase were colocalized within all of the peroxisomes. These consistent observations strongly suggest that the expressed peroxin sorts to pre-existing peroxisomes.

Another set of time-course experiments were done to assess trafficking of transiently expressed *myc*AtPEX16 to pre-existing peroxisomes marked with an endogenous PMP, namely APX. At 2 h, *myc*AtPEX16 was in perinuclear and cytoplasmic reticular ER (Fig. 2A, G) similar to that shown for *myc*AtPEX16 in Fig. 1C, Q that colocalized with representative ER markers illustrated in Fig. 1E, S. Solid arrowheads in Fig 2B, H point to representative pre-existing peroxisomes bearing endogenous APX; at 2 h post-bombardment, these peroxisomes do not possess *myc*AtPEX16 (Fig. 2A, G). At 2.5 h, *myc*AtPEX16 was observed in the ER of some of the transformed cells, but more frequently at this transition time period, *myc*AtPEX16 was observed within numerous non-peroxisomal punctate structures, i.e. without endogenous APX (compare C, D and I, J in Fig. 2). These images of

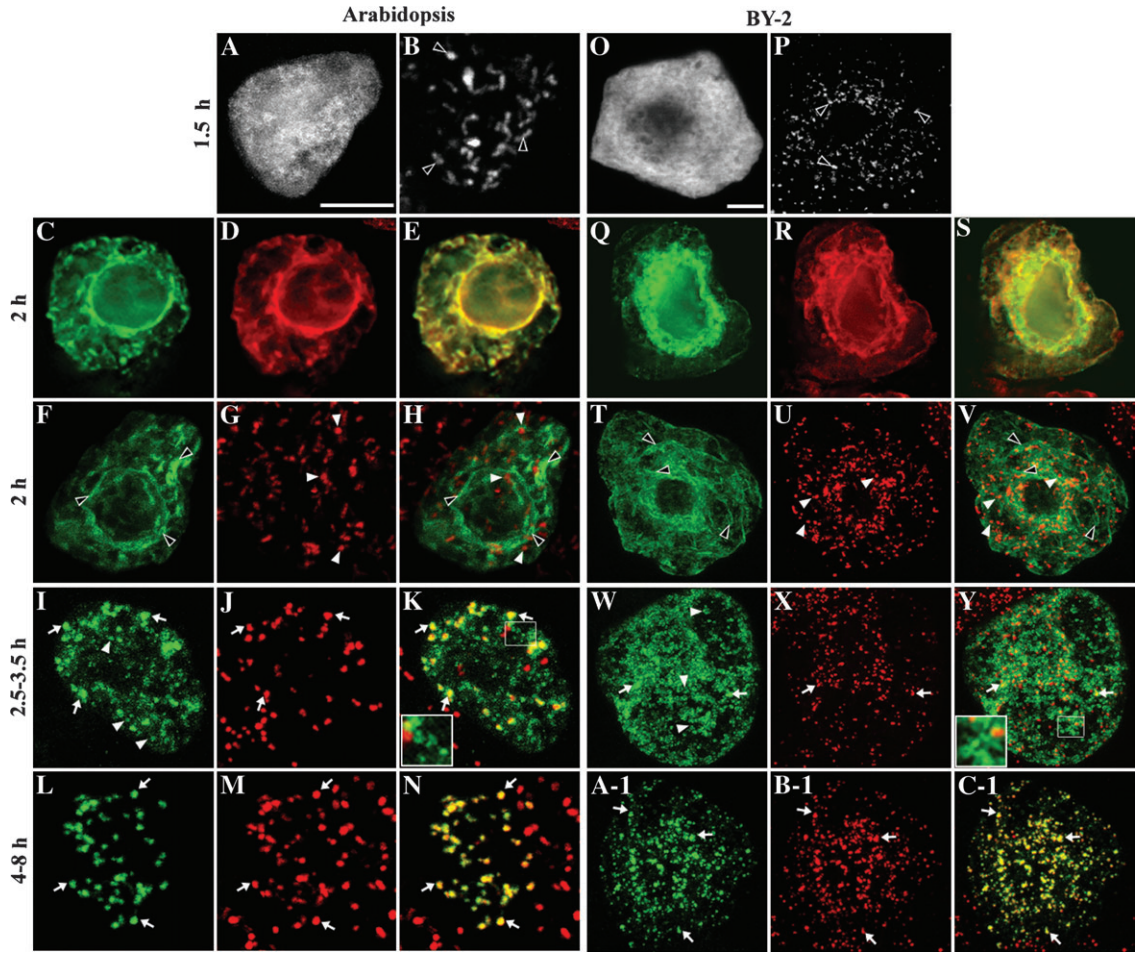

Fig. 1. Transiently expressed *myc*AtPEX16 trafficks indirectly from the cytosol to all of the catalase-containing (pre-existing) peroxisomes through the ER and a non-peroxisomal intermediate compartment in both *Arabidopsis* (A–N) and tobacco BY-2 (O–C-1) suspension cells. Cells biolistically bombarded with *myc*At*PEX16* were formaldehyde fixed at varied time points (left-side labels) and then dual immunolabelled with mouse anti-*myc* and rabbit anti-catalase or calnexin antibodies. (A, B, O, P) Cells labelled with anti-*myc* (A, O) and anti-catalase (B, P) IgGs; arrowheads point to peroxisomes, which are not apparent in *myc*-labelled cells. (C–E, Q–S) Bound anti-*myc* IgGs (green, C, Q) and anti-calnexin antibodies (red, D, R) are colocalized (yellow) within perinuclear and cytoplasmic reticular ER (merged images E and S). (F–H, T–V) Different cells are shown from the same 2 h group of cells. Cells labelled with anti-*myc* (green, F, T) and anti-catalase (red, G, U) antibodies; arrowheads highlight sites of non-colocalized antibodies (merged images H and V). (I–K, W–Y) Cells labelled with anti-*myc* (I, W) and anti-catalase (J, X) antibodies. Arrowheads point to punctate, non-peroxisomal structures (enlarged within insets from regions marked in the whole cells). Arrows point to catalase in peroxisomes colocalized with *myc*AtPEX16 that are distinct from *myc*-labelled non-peroxisomal structures (merged cell images and insets, K and Y). (L–N, A-1–C-1) Cells labelled with anti-*myc* (L, A-1) and anti-catalase (M, B-1) antibodies; arrows depict peroxisomal colocalizations of these antibodies (N and C-1, merged images). All panels are representative non-confocal epifluorescence images. Cy2-conjugated secondary antibodies marked bound anti-*myc* IgGs, and rhodamine-conjugated antibodies marked anti-catalase and anti-calnexin IgGs. Scale bars=10 μm.

varied structures are similar to those shown in Fig. 1I–K, W–Y. Significantly, at 5 h in both *Arabidopsis* and BY-2 cells, all pre-existing APX-containing peroxisomes possessed *myc*AtPEX16 (colocalizations represented by arrows in Fig. 2E, F, K, L).

Similar time-course experiments through 6 h post-bombardment were done with three other transiently expressed versions of AtPEX16, namely C-terminal *myc*-tagged, and N- and C-terminal-appended GFP constructs. Results were the same as described above, thus none of these data are shown. Of significance, particularly for later-described targeting experiments, the time-course events illustrated and described in Figs 1 and 2 were not as consistently co-ordinated in BY-2 cells as they were in *Arabidopsis* cells. This was also the case with all of the varied constructs employed. For example, at a given time point between 2 h and 6 h, *myc*AtPEX16 in some BY-2 cells on a microscope slide was observed solely in ER, the unidentified punctate structures, or in peroxisomes, whereas in other BY-2 cells on the slide, *myc*AtPEX16 appeared within all of these compartments simultaneously within the same cells. These results did not alter the interpretations of the images and time-course events presented above. Controls for all of these experiments included

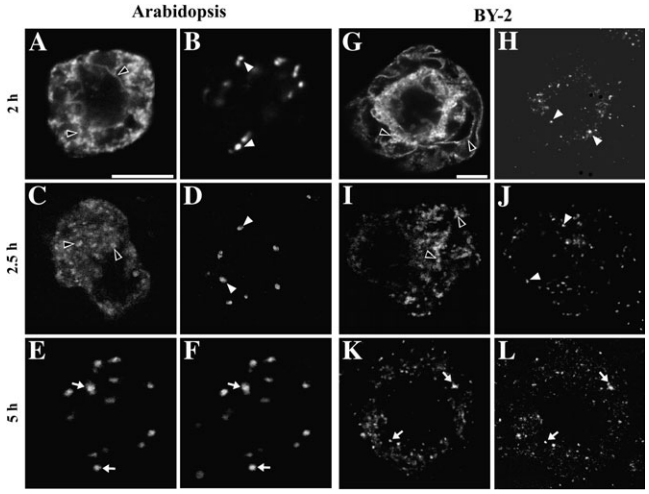

Fig. 2. Transiently expressed *myc*AtPEX16 trafficks indirectly to all of the APX-bearing (pre-existing) peroxisomes through the ER and a non-peroxisomal intermediate compartment in both *Arabidopsis* (A–F) and BY-2 (G–L) suspension cells. Cells biolistically bombarded with *myc*At*PEX16* were fixed at 2, 2.5, or 5 h and dual immunolabelled with mouse anti-*myc* (A, C, E, G, I, K) and rabbit anti-APX (B, D, F, H, J, L) antibodies. Arrowheads depict non-colocalizations in the same, single transformed cells. Arrows point to representative colocalizations of expressed *myc*AtPEX16 with endogenous APX in peroxisomes in the same, single transformed cells. All panels are images of representative confocal optical sections. Cy2-conjugated secondary antibodies marked bound anti-*myc* IgGs, and Cy5-conjugated antibodies marked anti-APX IgGs. Scale bars=10 μm.

omissions and substitutions (irrelevant antibodies) of the primary and/or secondary antibodies (data not shown).

Cold treatment halts trafficking of transiently expressed myc*AtPEX16 within the ER prior to its ultimate sorting to pre-existing peroxisomes*

As a means to dissect and elucidate further the indirect trafficking of nascent *myc*AtPEX16 to pre-existing peroxisomes, trafficking along this pathway was temporarily disrupted. Figure 3 is a grouping of representative images illustrating influences on the trafficking pattern of *myc*AtPEX16 expressed in cells subjected to 15 °C for 5 h and subsequently re-equilibrated at 25 °C. In control cells maintained at 25 °C for 5 h post-bombardment, nascent *myc*AtPEX16 sorted as previously shown to all of the catalase-containing pre-existing *Arabidopsis* and BY-2 peroxisomes (Fig. 3A, B, L, M). Maintaining bombarded cells at 15 °C for 5 h yielded significantly different results. Rather than sort to the normal-appearing catalase-containing peroxisomes in these cells (Fig. 3D, O), *myc*AtPEX16 accumulated within a reticular compartment distributed throughout the cytoplasm in both cell types (Fig. 3C, N). Identification of this compartment as reticular ER is shown by the virtually perfect colocalizations of *myc*AtPEX16 with endogenous calnexin in both cell types (Fig. 3E, F, P, Q). Notably, *myc*AtPEX16 did not accumulate in perinuclear ER at 15 °C as it did in cells held for 2 h at 25 °C (Fig. 1C–E, Q–S).

It was of interest to learn whether the *myc*AtPEX16 accumulated throughout the ER could travel with fidelity to the pre-existing peroxisomes. Figure 3G, H, R, S shows that after re-equilibration for 6 h at 25 °C, *myc*AtPEX16 occurred exclusively within all of the catalase-containing peroxisomes in transformed *Arabidopsis* and BY-2 cells. Edges of nearby non-transformed cells with peroxisomes are evident in Fig. 3H, S.

As a positive control for protein accumulation at 15 °C of a known ER secretory protein within the ER, experiments were conducted with cells transiently expressing GmMan1::(GFP), which was known to traffick though ER to Golgi bodies in BY-2 cells at 25 °C (Nebenführ *et al*., 1999; Lisenbee *et al*., 2003*b*). As expected, at 25 °C (5 h post-bombardment) GmMan1::(GFP) was localized in a punctate pattern indicative of Golgi bodies distributed throughout the cytoplasm of both cell types (Fig. 3I, T). The substantially fewer and larger Golgi bodies in *Arabidopsis* suspension cells compared with those in BY-2 cells have been described previously (Hawes, 2005). Incubation of bombarded cells at 15 °C (for 5 h) resulted in the accumulation of GmMan1::(GFP) in a reticular compartment observed throughout the cytoplasm of the confocal images (Fig. 3J, U). Perfectly colocalized autofluorescent GFP images with immunofluorescence calnexin images in transformed cells showed that this compartment was ER (data not shown). Shifting the cells maintained at 15 °C (5 h) to 25 °C and holding them for 6 h resulted in trafficking of GmMan1::(GFP) exclusively to Golgi bodies (Fig. 3K, V; images similar to 25 °C controls presented in Fig. 3I, T). Collectively, these results show that transiently expressed peroxisomal and secretory proteins accumulate throughout the reticular ER in cells held at 15 °C, and retain their capability for correctly sorting at 25 °C ultimately to their target organelles (Golgi bodies and peroxisomes).

Low temperature experiments were also used to acquire more information on the post-ER intermediate compartment described earlier (Figs 1I–K, W–Y, and 2C, I). Cells transferred from 15 °C (after 5 h) to 25 °C were fixed for immunofluorescence microscopy at intervals of 0.5, 1.0, 1.5, and 2.0 h. Surprisingly, at 0.5 and 1.0 h, *myc*AtPEX16 remained localized mainly within reticular ER (data not shown). At 1.5 h, the first significant changes in subcellular localization were observed. *myc*AtPEX16 was observed mainly in punctate, variably shaped structures (Fig. 4A, G), which were reminiscent of those observed during the normal time-course of events at 25 °C illustrated in Fig. 1K, Y (and insets) and in Fig. 2C, I. The anti-*myc* immunofluorescence signals emanating from these structures did not colocalize (arrowheads) with anti-catalase immunofluorescence derived from peroxisomes (compare A, B and G, H in Fig. 4). Another portion of these transformed cells examined after 1.5 h at 25 °C were dual immunolabelled with anti-*myc* and anti-Sec21 antibodies. Sec21 is a constituent protein of the COPI

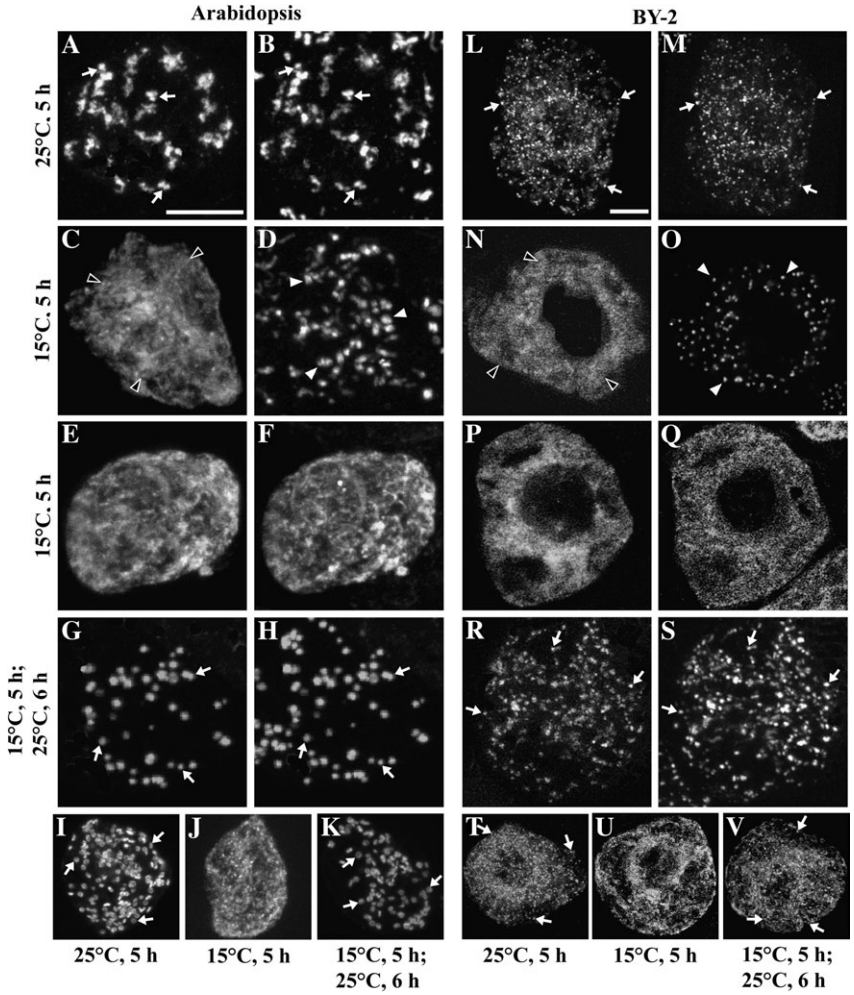

Fig. 3. Transiently expressed *myc*AtPEX16 accumulates in ER at 15 °C (5 h) and then moves to the catalase-bearing pre-existing peroxisomes (not Golgi bodies) after re-equilibrations at 25 °C in both *Arabidopsis* (A–H) and BY-2 (L–S) suspension cells. Cells biolistically bombarded with *myc*At*PEX16* (A–H, L–S) or GmMan1::(GFP) (I–K, T–V) were incubated either at 25 °C for 5 h (A, B, L, M, I, T) or at 15 °C for 5 h (C–F, N–Q, J, U). A group of cells held at 15 °C for 5 h subsequently were incubated at 25 °C for 6 h (G, H, R, S, K, V). (A–D, L–O) Cells dual labelled with anti-*myc* (A, C, L, N) and anti-catalase (B, D, M, O) antibodies; arrows point to representative sites of colocalizations, whereas arrowheads highlight representative non-colocalizations. (E, F, P, Q) Anti-*myc* (E, P) antibodies are colocalized anti-calnexin (F, Q) IgGs. (G, H, R, S) Cells dual labelled with anti-*myc* (G, R) and anti-catalase (H, S) antibodies; arrows show colocalizations. (I–K, T–V) Autofluorescence from GmMan1::(GFP) in transformed cells; arrows point to Golgi bodies. All images are confocal projections, most from the entire cell; (N–Q) are from the middle of the cell. Cy2-conjugated secondary antibodies marked bound mouse anti-*myc* IgGs, and Cy5-conjugated antibodies marked rabbit anti-catalase and anti-calnexin IgGs. Scale bars=10 μm.

coatomer in Golgi vesicles. Figure 4C, D, I, J shows that the *myc*AtPEX16 signals in the punctate structures (Fig. 4C, I) were not colocalized with anti-Sec21 antibody signals marking Golgi bodies (Fig. 4D, J). At 2.0 h post-shift to 25 °C from 15 °C, *myc*AtPEX16 was localized mainly in peroxisomes (data not shown).

That these anti-Sec21 antibodies recognize Golgi bodies in both *Arabidopsis* and BY-2 cells was shown in a separate transformation experiment (Fig. 4E, F, K, L). The autofluorescent signal from transiently expressed GmMan1::(GFP) at 5 h post-bombardment (Fig. 4E, K) perfectly colocalized with the anti-Sec21 immunofluorescence within endogenous Golgi bodies.

BFA treatments interrupt trafficking of transiently expressed myc*AtPEX16 through the ER to pre-existing peroxisomes*

The third set of experiments conducted to dissect the trafficking pathway of nascent *myc*AtPEX16 entailed evaluations of incubations of cells in BFA, which is known to interfere indirectly with the normal exit of proteins from the plant ER; the mechanism(s) for the block are discussed later. Figure 5 is a grouping of representative images illustrating results of these experiments. In a control treatment, bombarded cells were plated on filter paper for 5 h with medium containing 10% (v/v) DMSO (used to dissolve BFA). As expected, transiently

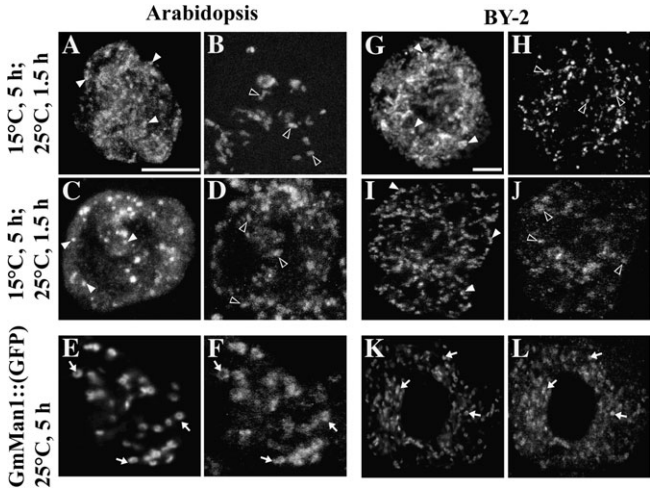

Fig. 4. Transiently expressed *myc*AtPEX16 accumulates in ER for 5 h at 15 °C, and after re-equilibration for 1.5 h at 25 °C is observed within a non-peroxisomal, non-Golgi body intermediate compartment in *Arabidopsis* (A–F) and BY-2 (G–L) cells. (A–D, G–J) Cells held at 15 °C for 5 h were transferred to 25 °C and held for 1.5 h, then fixed in formaldehyde and dual labelled for immunofluorescence microscopy. (E, F, K, L) Cells bombarded with genes coding for GmMan1::(GFP) were fixed after 5 h expression, and single immunolabelled. (A, B, G, H) Cells labelled with anti-*myc* (A, G) and anti-catalase (B, H) antibodies; arrowheads depict representative non-colocalizations. (C, D, I, J) Cells labelled with anti-*myc* (C, I) and anti-Sec21 (D, J) antibodies; arrowheads highlight representative non-colocalizations. (E, F, K, L) Cells exhibiting GFP autofluorescence from transiently expressed GmMan1::(GFP) (E, K) and Cy5 fluorescence from secondary antibodies bound to anti-Sec21 (F, L); arrows show obvious colocalizations between the two Golgi markers in both cell types. All images are confocal projections composed of optical sections from the middle area of the cells. Secondary antibodies were conjugated to Cy2 for anti-*myc,* and to Cy5 for anti-catalase and anti-Sec21 primary antibodies. Scale bars=10 μm.

expressed *myc*AtPEX16 was localized exclusively within all of the catalase-containing pre-existing peroxisomes in both *Arabidopsis* and BY-2 cells (Fig. 5A–C, M–O). Upon plating similar cells for 5 h in BFA-containing medium, expressed *myc*AtPEX16 was not observed within the peroxisomes (Fig. 5D–F, P–R). Instead, *myc*AtPEX16 accumulated in a reticular compartment distributed throughout the cytoplasm of both cell types (Fig. 5F, R). The reticular compartment was identified as ER from the near perfect colocalizations with endogenous calnexin (Fig. G–I, S–U). Note that perinuclear ER was not visualized. After BFA-treated cells were transferred to plates with BFA-free medium for 6 h, *myc*AtPEX16 was detected only in peroxisomes in both cell types (Fig. 5J–L, V–X).

The tripeptide -VRS- and the upstream membrane helix 1 are necessary for sorting nascent myc*AtPEX16 through the ER to peroxisomes*

Previously, it had been reported by Karnik and Trelease (2005) that AtPEX16 has two internal membrane helices (MH1, MH2; residues 237–256 and 264–284, respectively) and three clusters of basic residues near these MHs (residues 219–225, 257–264, and 306–310) (see also diagrammatic scheme in Table 2). This grouping of MHs and basic-charged residues resembled the prototypic membrane peroxisome targeting signal (mPTS) found in most other PMPs (Sparkes and Baker, 2002; Van Ael and Fransen, 2006). To determine which, if any, of these group(s) of residues in AtPEX16 conferred minimally necessary ER and/or peroxisomal targeting information, they were independently deleted or altered in *myc*AtPEX16 (Table 2). As noted above, images of BY-2 cells (at 5 h post-bombardment) characteristically showed multiple subcellular localizations within the same cell. This was an advantageous feature compared with *Arabidopsis* cells, since sorting (direct or indirect) from the cytosol to peroxisomes could be determined from examinations of the individual BY-2 cells. Comparative distinctions in *Arabidopsis* cells required examining bombarded cells fixed and processed at 2 h and 5 h.

Table 2 lists all of the mutated versions of *myc*AtPEX16, GFPm constructs, and localization results for this part of the study. However, only selected immunofluorescence images are presented in Figs 6 and 7.

As a basis for comparisons, Fig. 6A, B, M, N shows at 5 h post-bombardment the characteristic localizations for *myc*AtPEX16 exclusively in *Arabidopsis* peroxisomes (Fig 6A, B), and in both reticular ER (arrowheads) and peroxisomes (arrows) in BY-2 cells (Fig. 6M, N). Images of the BY-2 cells are presented as pseudo-coloured images so that readers can distinguish between the two compartments. The same localizations were found for expressed *myc*AtPEX16Δ79, a construct with deletion of the C-terminal 79 residues that included the basic cluster at position 306–310 (Fig. 6C, D, O, P). Similar results were observed with the *myc*AtPEX16Δ87 construct (Table 2; images not shown). Removal of the MH2 at position 265–279 along with the basic cluster at position 306–310, both within the C-terminal 102 residues, did not change the targeted localizations (Fig. 6E, F, Q, R).

Sorting, however, of *myc*AtPEX16 to ER and/or peroxisomes was abolished upon deletion of four more residues, i.e. the C-terminal 106 amino acid residues that included residues VRS at position 262–264 along with MH2 and the basic cluster at position 306–310. Nascent *myc*AtPEX16Δ106 accumulated throughout the cytosol of both plant cells (Fig. 6G, S), not the peroxisomes (Fig. 6H, T) or ER identified with anti-calnexin IgGs (images not shown). As expected, cytosolic accumulations also were observed in both cells when *myc*AtPEX16Δ111, *myc*AtPEX16Δ134, and *myc*AtPEX16Δ148 were transiently expressed for 5 h (Table 2; images not shown).

To test whether targeting to ER and/or peroxisomes required certain, specific basic residues, the tri-arginine residues at position 306–308, and separately at position 221–223, were substituted with three glycine residues.

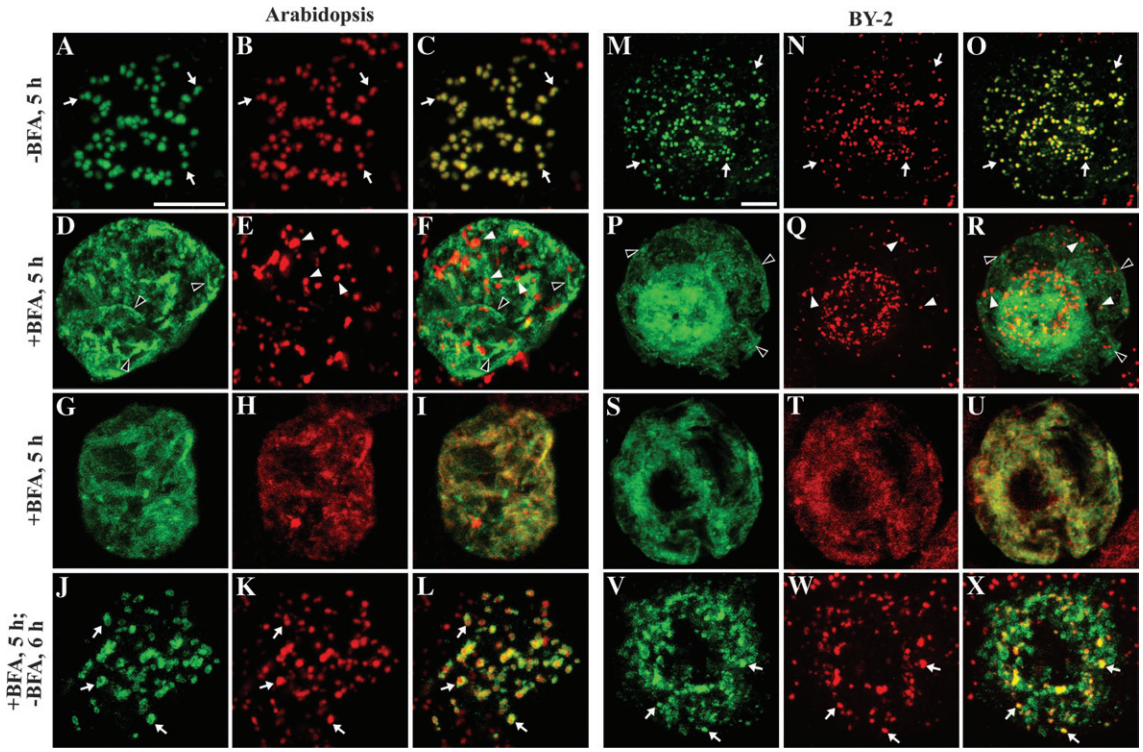

Fig. 5. Transiently expressed *myc*AtPEX16 accumulates within reticular ER in the presence of BFA and, following removal of BFA, moves to all of the catalase-containing pre-existing peroxisomes in both *Arabidopsis* (A–L) and BY-2 (M–X) cells. Cells bombarded with *myc*At*PEX16* were held on plates for 5 h at 25 °C in transformation medium containing DMSO (A–C, M–O) or BFA (D–I, P–U). Cells on some of the BFA-treated plates were washed and re-plated in medium without BFA and held for 6 h at 25 °C (J–L, V–X). (A–C, M–O) Cells dual immunolabelled with anti-*myc* (A, M) and anti-catalase (B, N) antibodies; arrows depict typical sites of peroxisomal colocalizations emphasized in yellow in the merged images C and O. (D–F, P–R) Cells dual labelled with anti-*myc* (D, P) and anti-catalase (E, Q) antibodies; arrowheads point to representative non-colocalizations most distinctly evident in merged images (F) and (R). (G–I, S–U) Cells dual labelled with anti-*myc* (G, S) and anti-calnexin (H, T) antibodies; colocalizations (yellow) are apparent reticular structures in merged images (I, U). (J–L, V–X) Cells dual labelled with anti-*myc* (J, V) and anti-catalase (K, W) antibodies; arrows point to peroxisome colocalizations emphasized in yellow in merged cells (L, X). Images are confocal projections, mostly from the middle areas of the cells. Secondary antibodies were conjugated to Cy2 for anti-*myc*, and to Cy5 for anti-catalase and anti-calnexin primary antibodies. Scale bars=10 μm.

These substitutions did not affect targeting in either cell type (Table 2). Similarly, substitutions of arg-lys-tyr at positions 258–260 with glycine residues permitted sorting of *myc*AtPEX16RKY(258–260)ΔGGG to *Arabidopsis* peroxisomes (Fig. 6I, J) and to BY-2 ER and peroxisomes (Fig. 6U, V). However, upon substitution of all seven of the residues at position 258–264 with glycine, *myc*AtPEX16RKYGVRSΔ7G accumulated in the cytosol of both cell types (Fig. 6K, W), not targeted to *Arabidopsis* peroxisomes or BY-2 ER/peroxisomes (Fig. 6L, X).

Membrane helices 1 and 2 (MH 1 and 2) and the intervening amino acid sequence including a cluster of basic residues in AtPEX16 are sufficient for sorting GFP to peroxisomes via the ER

To ascertain which amino acid residues and/or (sub)domains were sufficient for organellar targeting, gene constructs were built with different portions of the At*PEX*16 gene appended to the 3' end of GFPm DNA, creating a gene coding for the heterologous reporter protein GFPmAtPEX16 (Table 2). Figure 7 is a grouping of representative images illustrating the localizations of these fusion constructs at 5 h post-bombardment. The images in the top row were not pseudo-coloured since clarity of localizations was obscured rather than enhanced. In control experiments, GFPm alone was localized within the cytosol and nucleus in both *Arabidopsis* and BY-2 cells (Fig. 7A, M). GFPmAtPEX16211–237, which included tri-arginine residues (221–223) within a group of other basic residues, but not MH1, accumulated in the cytosol (images not shown). Figure 7B, N shows that construct GFPmAtPEX16211–256, which included these basic residues at position 219–225 and MH1, also accumulated within the cytosol and nucleus. GFPmAtPEX16211–261 with MH1 and basic resides at 219–225 also accumulated in the cytosol (images not shown). Figure 7C, O shows GFPmAtPEX16211–265, which includes MH1 along with the basic residues at positions 219–225 and 257–264, also accumulated in the

Table 2. *Localization of AtPEX16 targeting constructs in* Arabidopsis *and Bl-2 cells*

Protein code	Targeting construct	Localization	
		Arabidopsis	BY-2
*myc*AtPEX16		Peroxisomes	ER,Peroxisomes
*myc*AtPEX16Δ79		Peroxisomes	ER,Peroxisomes
*myc*AtPEX16Δ87		Peroxisomes	ER,Peroxisomes
*myc*AtPEX16Δ102		Peroxisomes	ER,Peroxisomes
*myc*AtPEX16Δ106		Cytosol	Cytosol
*myc*AtPEX16Δ111		Cytosol	Cytosol
*myc*AtPEX16Δ134		Cytosol	Cytosol
*myc*AtPEX16Δ148		Cytosol	Cytosol
*myc*AtPEX16RRR(306-308)ΔGGG		Peroxisomes	ER,Peroxisomes
*myc*AtPEX16RRR(221-223)ΔGGG		Peroxisomes	ER,Peroxisomes
*myc*AtPEX16RKY(258-260)ΔGGG		Peroxisomes	ER,Peroxisomes
*myc*AtPEX16RKYGVRS(258-264)Δ7G		Cytosol	Cytosol
GFPm	GFPm	Cytosol	Cytosol
GFPmAtPEX16 211-237	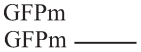	Cytosol	Cytosol
GFPmAtPEX16 211-256	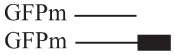	Cytosol	Cytosol
GFPmAtPEX16 211-261	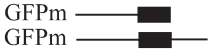	Cytosol	Cytosol
GFPmAtPEX16 211-265		Cytosol	Cytosol
GFPmAtPEX16 211-279		ER,Peroxisomes	ER,Peroxisomes
GFPmAtPEX16 211-310		ER,Peroxisomes	ER,Peroxisomes
GFPmAtPEX16 257-279		Cytosol	Cytosol
GFPmAtPEX16 235-279		ER,Peroxisomes	ER,Peroxisomes
GFPmAtPEX16		ER,Peroxisomes	ER,Peroxisomes

cytosol and nucleus, as evidenced by non-colocalizations in the same cells with endogenous catalase (Fig. 7D, P) and non-colocalizations with endogenous calnexin (data not shown).

Construct GFPmAtPEX16211–279 that included MH1 and MH2 along with the basic residues at positions 219–225 and 257–264 sorted to the ER (arrowheads in Fig. 7E, Q) and peroxisomes (arrows in Fig. 7E, Q) as evidenced by colocalizations with endogenous catalase (Fig. 7F, R) and endogenous calnexin (data not shown). Similar results were observed with construct GFPmAtPEX16211–310 that included all the three basic domains as well as MH1 and MH2 (Fig. 7G, H, S, T). However, construct GFPmAtPEX16257–279, that included basic residues at position 257–264 and MH2, was localized in the cytosol (Fig. 7I, U) as evidenced by non-colocalizations with endogenous catalase (Fig. 7J, V). Construct GFPmAtPEX16235–279, which included basic residues at positions 257–264 along with MH1 and MH2, but not basic residues at 219–225, was localized in the ER (arrowheads in Fig 7K, W,) and the peroxisomes (arrows in Fig. 7L, X).

Collectively, the results presented in Table 2 and Fig. 7 show that both MH1 and MH2 and the intervening residues that include the basic cluster of residues at position 257–264 were minimally sufficient for targeting GFPm to ER and then to peroxisomes.

Discussion

In a previous study (Karnik and Trelease, 2005), it was found that the *Arabidopsis* PEX16 homologue was an endogenous membrane protein that existed at steady state not only in peroxisomes of *Arabidopsis* suspension cells, but also throughout the ER of these cells. These findings were of particular importance with regard to the 'early peroxin' function of AtPEX16 (Lin *et al*., 2004; Karnik and Trelease, 2005) and to the resurgence of ER participation in the biogenesis of peroxisomes in all organisms (Kunau, 2005; Kim *et al*., 2006; Titorenko and Mullen, 2006; Trelease and Lingard, 2006; van der Zand *et al*., 2006). In the current study, the hypothesis that AtPEX16 was dynamically linked between the ER and peroxisomes in *Arabidopsis* as well as in tobacco BY-2 cells was tested. Results from the time-course experiments, which included different experimental treatments that impaired protein trafficking through the ER, supported our hypothesis. Our interpretations of the data were that nascent epitope-tagged *myc*AtPEX16 was sorted post-translationally via internal molecular targeting signal(s) from the cytosol through the ER and an ERPIC to pre-existing peroxisomes. An ERPIC had been portrayed in several biogenesis models (Mullen *et al*., 2001*a*; Mullen and Trelease, 2006; Trelease and Lingard, 2006), but not actually identified previously in any plant cell. Specific molecular targeting signal(s) were postulated for directing

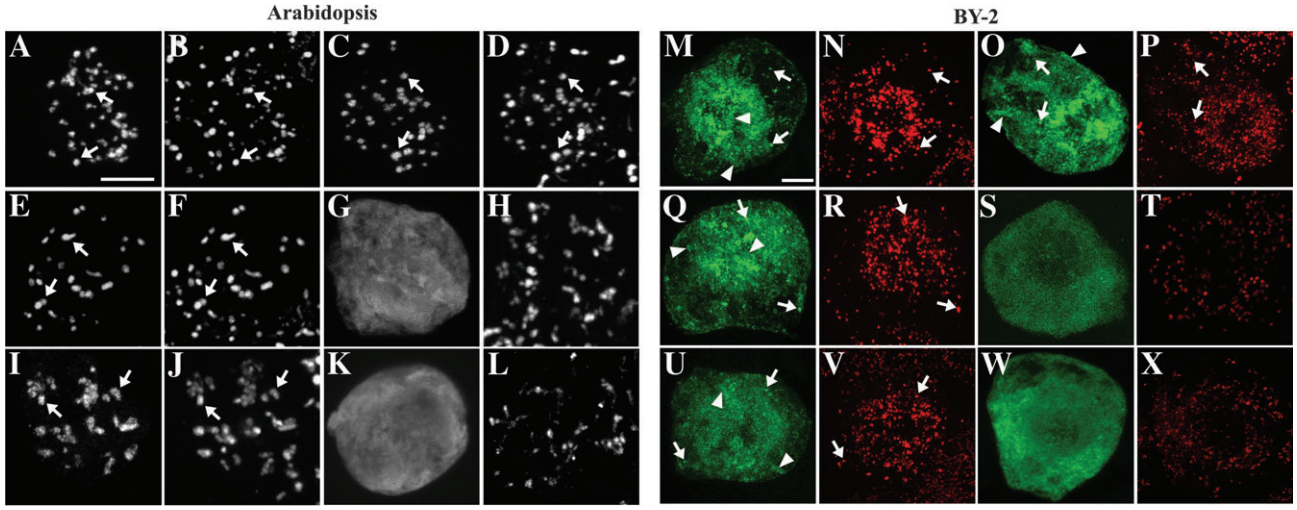

Fig. 6. MH1 and downstream amino acid residues -VRS- adjacent to MH2 are necessary for targeting transiently expressed *myc*AtPEX16 to the ER and then to the peroxisomes in *Arabidopsis* and BY-2 cells. Cells expressing unaltered or modified versions of *myc*AtPEX16 at 5 h post-bombardment were dual immunolabelled with anti-*myc* IgGs (A, C, E, G, I, K, M, O, Q, S, U, W) and anti-catalase (all other panels) IgGs. (A and M, C and O, E and Q, G and S, I and U, K and W) Immunofluorescence attributable to transiently expressed *myc*AtPEX16, *myc*AtPEX16Δ79, *myc*AtPEX16Δ102, *myc*AtPEX16Δ106, *myc*AtPEX16RKY(258–260)ΔGGG, *myc*AtPEX16RKYGVRS(258–264)Δ7G, respectively. (B and N, D and P, F and R, H and T, J and V, L and X) Catalase-labelled peroxisomes in the same corresponding transformed cells. Arrows point to representative sites of colocalizations in both cell types; arrowheads indicate representative non-colocalization sites in BY-2 cells. Due to the more numerous and smaller peroxisomes in BY-2 cells, these images were pseudo-coloured for clarity. All panels are representative confocal projections. Secondary antibodies were conjugated to Cy2 for anti-*myc*, and to Cy5 for anti-catalase primary antibodies. Scale bars=10 μm.

*myc*AtPEX16 through this indirect pathway to the peroxisomes. However, separate non-overlapping organellar signals were not discovered, although a minimally essential internal triplet of basic amino acid residues was necessary, but not sufficient, for trafficking *myc*AtPEX16 and GFPm, respectively, to the peroxisomes.

Evidence for sorting of nascent myc*AtPEX16 from the cytosol to peroxisomes*

In an earlier study, Sparkes *et al*. (2005) set out to determine experimentally whether two other nascent over-expressed peroxins, namely AtPEX2 and AtPEX10, sorted to peroxisomes directly from the cytosol, or indirectly through cytoplasmic ER. In this endeavour, they were concerned with distinguishing cytosolic fluorescence images from cytoplasmic-ER fluorescence images in tobacco leaf epidermal cells. Their approach was simultaneously to compare fluorescence images of the overexpressed chimeric peroxins with free YFP signals known to be in the cytosol. They concluded that both of these peroxins by-passed the ER and sorted directly from the cytosol to pre-existing tobacco peroxisomes.

The immunofluorescence images obtained at early time periods in the current control time-course experiments (Fig. 1) were interpreted as evidence for nascent, transiently expressed *myc*AtPEX16 appearing first in the cytosol of both cell types (1.5 h, Fig. 1A, O) and then moving post-translationally to the ER (2 h, Fig. 1C–E, Q–S). As was the case for Sparkes *et al*. (2005), it was important for us reliably to determine whether *myc*AtPEX16 at these time points was located in cytoplasmic ER and/or in the cytosol. This was greatly facilitated by using single suspension-cultured cells compared with assessing images of tissue cells in whole plant parts.

One of the distinguishing features was that the *myc*AtPEX16 observed in the putative cytoplasmic ER exhibited a reticular appearance compared with the more uniform image of *myc*AtPEX16 interpreted to be expressed in the cytosol (compare A, C and O, Q in Fig. 1). More convincing, however, was the appearance of expressed *myc*AtPEX16 concentrated also in the perinuclear region that colocalized with the ER marker calnexin (Fig. 1E, S). Perinuclear immunofluorescence was not observed in apparent cytosolic-localized *myc*AtPEX16 (compare A, C and O, Q in Fig. 1). Furthermore, recognition of cytosolic-localized proteins was inherent in the current molecular targeting experiments. Hundreds of observations were made on microscope slides of modified *myc*AtPEX16 constructs mistargeted to the non-perinuclear cytosol (see examples in Figs 6 and 7). Finally, the site of expressed proteins in the cytosol was most obvious in the current sufficiency experiments wherein mistargeted cytosolic GFPm constructs characteristically appeared within the cytosol and the nucleus (see examples in Fig. 7). The passive diffusion of soluble GFP from the cytosol through nuclear pores into the nucleoplasm is widely accepted.

These assessments of numerous images supported our contention that nascent *myc*AtPEX16 sorted at early time periods of expression from its site of synthesis in the

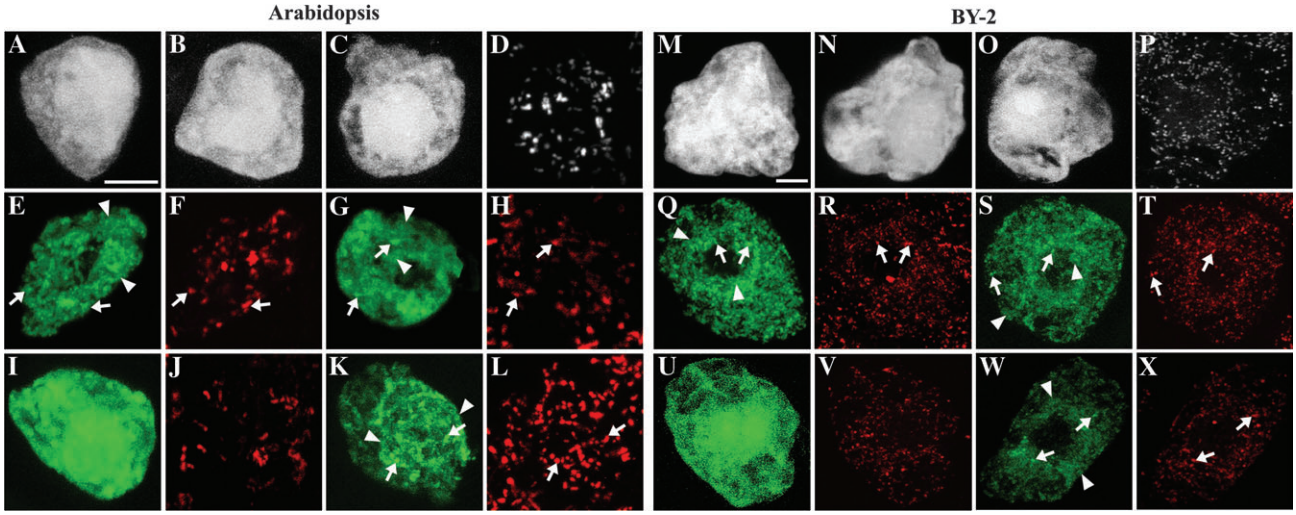

Fig. 7. Two internal membrane helices (MH1 and MH2) and the intervening residues including the cluster of basic amino acid residues (IRKYGVRS) are sufficient for targeting transiently expressed heterologous AtPex16–GFPm constructs to the ER and then to peroxisomes in *Arabidopsis* and BY-2 cells. Cells expressing different portions of AtPEX16 fused to the C-terminus of GFPm were immunolabelled with anti-catalase IgGs shown in red D, F, H, J, L, P, R, T, V, X (pseudo-coloured in red except D and P). (A and M, B and N, C and O) Autofluorescence in the cytosol and nucleus attributable to GFPm, GFPmAtPEX16211–256, and GFPmAtPEX16211–265, respectively. (D and P) Endogenous catalase in peroxisomes in the same GFPmAtPEX16211–265 transformed cell shown in C and O, respectively. Pseudo-coloration of these images obscured the observations. (E and Q, G and S, I and U, K and W) Autofluorescence (green) exhibited by GFPmAtPEX16211–279, GFPmAtPEX16211–310, GFPmAtPEX16257–279, and GFPm235–279, respectively. (F and R, H and T, J and V, L and X) Catalase-labelled peroxisomes (red) in the same corresponding transformed cells. Arrows point to representative sites of colocalizations; arrowheads indicate representative non-colocalization sites. All panels are representative confocal projections. Secondary antibodies were conjugated to Cy5 for marking primary anti-catalase IgGs. Sclae bars=10 μm.

cytosol indirectly to peroxisomes through the ER (cytoplasmic reticular and perinuclear). Such evidence for indirect sorting, places AtPEX16 among the so-called Group I PMPs (Titorenko and Rachubinski, 2001*b*; Heiland and Erdmann, 2005; Kim *et al*., 2006; Titorenko and Mullen, 2006). Both of the other known PEX16 homologues, namely YlPEX16 in *Yarrowia lipolytica* (Titorenko and Rachubinski, 1998, 2000) and HsPEX16 in *Homo sapiens* cells (Kim *et al*., 2006) were considered as Group I PMPs, although HsPEX16 was classified as a Group II PMP in other studies where it was interpreted to travel from the cytosol directly to peroxisomes (South and Gould, 1999; Honsho *et al*., 2002). Interestingly, AtPEX16 joins AtPEX10 as only the second Group I peroxin that has been identified in plants; however, assignment of AtPEX10 to this group is controversial (Schumann *et al*., 2003; Flynn *et al*., 2005; Sparkes *et al*., 2005). AtPEX16 is only the third known Group I plant PMP, joining the viral protein p33 (McCartney *et al*., 2005) and the enzyme APX (Mullen and Trelease, 2000; Lisenbee *et al*., 2003*a*). At present there are many more known Group II plant PMPs that are listed or described in the papers and reviews (e.g. Trelease, 2002; Murphy *et al*., 2003; Hunt and Trelease, 2004, Sparkes *et al*., 2005; Lisenbee *et al*., 2005; Baker and Sparkes, 2005; Lingard and Trelease, 2006; Trelease and Lingard, 2006). A conceptual or specific reason for this difference in relative number is not readily apparent at this time.

Segregation and accumulation of myc*AtPEX16 within the cytoplasmic reticular ER*

Considering the previously demonstrated steady-state existence of endogenous AtPEX16 throughout the reticular ER, questions arose as to whether transiently overexpressed *myc*AtPEX16 would sort through the ER *en route* to peroxisomes and, if so, would *myc*AtPEX16 appear throughout the ER, or appear only at the peroxisomal ER subdomain(s) as does transiently overexpressed *HA*-APX in BY-2 cells (Mullen *et al*., 1999, 2001*b*; Lisenbee *et al*., 2003*a*, *b*). As mentioned above, *myc*AtPEX16 became distributed throughout the reticular and perinuclear ER in both *Arabidopsis* and BY-2 cells (Figs 1 and 2). Thus, *HA*-APX and *myc*AtPEX16 segregate differently within the ER. A definitive reason for this difference has not been resolved, although it is likely that it is correlated with the proposed multiple functions for AtPEX16 in the ER and peroxisomes (Lin *et al*., 1999, 2004; Guo *et al*., 2003; Karnik and Trelease, 2005; Brocard *et al*., 2005; Kim *et al*., 2006) versus the single enzymatic function for APX in peroxisomes (Bunkelmann and Trelease, 1996; Corpas and Trelease, 1998; del Rio *et al*., 2002, 2006).

Modifications of the normal time-course were made to experimentally disrupt the ER in ways that were intended to temporarily block (halt) protein trafficking through the ER. If *myc*AtPEX16 were dynamically (and quickly) moving through the ER *en route* to peroxisomes as

predicted, then *myc*AtPEX16 would accumulate within the ER, or subdomains thereof, and be readily observed via immunofluorescence microscopy. Alternatively, if *myc*AtPEX16 were a Group II PMP, then it would bypass all parts of the ER and be observed only in the peroxisomes.

The rationale for applying cold treatments to the plant suspension cells used in the current study came from several studies involving mammalian cells. Secretory proteins from the ER/Golgi intermediate compartment were blocked in cells incubated for several hours at 15 °C (Saraste and Kuismanen, 1984; Martinez-Alonso *et al*., 2005). Also, South and Gould (1999) reported that they did not find any significant inhibition of HsPEX16*myc* sorting to peroxisomes in PBD061 fibroblast cells that were incubated at 15 °C. They concluded that HsPEX16-*myc*, and ostensibly other PEX16 homologues, did not traffick to peroxisomes through the ER. In direct contrast, it was found in the current study that incubation of *Arabidopisis* or BY-2 cells at 15 °C clearly inhibited trafficking of *myc*AtPEX16 to peroxisomes as compared with cells maintained at, or returned to, 25 °C (Figs 3, 4). Perfect colocalizations of *myc*AtPEX16 with calnexin (Fig. 3E, F, P, Q) were convincing evidence that *myc*AtPEX16 accumulated within the plant cytoplasmic reticular ER.

Our interpretation is that the cold treatment (15 °C) results in a blockage, or significant slowing, of protein (*myc*AtPEX16) movement through the ER. Supportive evidence was that a plant secretory protein bound to GFP, specifically GmMan1::(GFP), which normally routes from the ER to Golgi bodies in *Arabidopsis* and BY-2 cells (Nebenführ *et al*., 1999), also accumulated within ER of cold-treated (15 °C) cells (Fig. 3J, U). Upon return of the cells to 25 °C, *myc*AtPEX16 and GmMan1::(GFP) (in different transformed cells) sorted exclusively to peroxisomes and Golgi bodies, respectively. The latter findings are a good indication that the accumulations observed in ER were not due to severe, cold-imposed cellular membrane damage (see discussion of perinuclear ER below). It has not been resolved why South and Gould (1999) did not observe HsPEX16*myc* accumulation in the mammalian cell ER, particularly since Kim *et al*. (2006) found that formation of new peroxisomes in mammalian cells was dependent upon ER-sorted HsPEX16.

The similar accumulation of *myc*AtPEX16 in the ER of BFA-treated cells (Fig. 5) is strong corroborative evidence for indirect sorting to the peroxisomes. BFA is known to inhibit COPI-coated vesicle formation at the Golgi cisternae (Nebenführ, 2002; Ritzenthaler *et al*., 2002; Yang *et al*., 2005). In plant cells, however, this effect leads indirectly to the blockage of protein exit from the ER. That is, a majority of the Golgi cisternae fuse with the ER creating a compromised trafficking hybrid compartment (Nebenführ, 2002). Hence, the accumulation of *myc*AtPEX16 in the ER (Fig. 5I, U) was probably due to the physical inability of ER-derived vesicles, or some other *myc*AtPEX16 membrane carriers, to exit the ER. In other studies, BFA-treatment experiments have been cited as evidence for certain proteins being either Group I PMPs (overexpressed *HA*-APX and endogenous APX; Mullen *et al*., 1999, 2001*b*; Lisenbee *et al*., 2003*a*) or Group II PMPs (AtPEX10 and AtPEX2; Sparkes *et al*., 2005). Upon removal of BFA in the current study, *myc*AtPEX16 ended up exclusively within peroxisomes (Fig. 5L, X). This was in accordance with the ER (and Golgi bodies) becoming re-established as separate entities, confirming previous conclusions that the physical ER blockage was a reversible, virtually innocuous event (Nebenführ, 2002).

An unexplained yet potentially significant observation was made in both BFA- and cold-treated cells. As predicted and discussed above, *myc*AtPEX16 accumulated throughout the cytoplasmic reticular ER, but unexpectedly did not appear within the perinuclear ER of either cell type. This phenomenon apparently was not due to the selective exclusion of *myc*AtPEX16 from existing perinuclear ER because application of anti-calnexin antibodies indicated that ER was not present in the perinuclear ER region of either cell type (Figs 3E, F, P, Q and 5I, U). We are unaware of any other report describing similar results. The observations suggest that the perinuclear ER was somehow selectively degraded. Interestingly, whatever happened to the perinuclear ER did not prevent correct subsequent sorting of the *myc*AtPEX16 PMP exclusively to peroxisomes during the recovery periods. This was somewhat surprising because of the prevalent occurrence of *myc*AtPEX16 in the perinuclear ER of untreated cells (Figs 1, 2). One possible effect that is considered in the following section is that the travel time of *myc*AtPEX16 from the ER to peroxisomes might have been slowed during the recovery periods.

Identification and characterization of ERPIC

A novel feature of the current time-course experiments was that images of *myc*AtPEX16 within an apparent non-peroxisomal, post-ER intermediate compartment were captured (Figs 1K, Y and 2C, I) referred to herein and in other studies generally as ERPIC (e.g. Titorenko and Mullen, 2006). The compartment is composed of variously sized structures observed most clearly in the single optical sections (e.g. Fig. 2C, I). We determined that *myc*AtPEX16 within the ERPIC was not co-localized with Golgi bodies possessing the marker Sec21p, or with Golgi-targeted GmMan1::GFP (Fig. 4C–F, I–L). At the present time, we interpret the ERPIC images as reflecting indiscriminant collections of membrane carriers composed possibly of vesicles and/or fragments (lamellae) (examples described in Geuze *et al*., 2003: van der Zand *et al*., 2006). These carriers might be derived and be in transit from portions of the ER or, alternatively, exist at steady state as an intermediate pre-existing compartment.

Although the current observations of *myc*AtPEX16 within the *Arabidopsis* ERPIC were made within a rather short temporal window of about 2.5–3.5 h, it was not possible to distinguish among the alternatives given above. An expectation was that better resolution of the structure and dynamics of the ERPIC could be obtained from the cold- and BFA-treatment experiments. The prediction was that *myc*AtPEX16 accumulated within the ER would, upon recoveries (BFA removal, return to 25 °C), move rapidly at high membrane concentrations into the ERPIC. Unfortunately, this did not occur during either recovery. *myc*AtPEX16 indeed appeared in the ERPIC, but only after a 1.5 h delay, and slowly over several hours (Fig. 4C, D, I, J). Although sorting fidelity to peroxisomes was maintained during the recoveries, re-organization of the disrupted ER, including the obvious effects on perinuclear ER discussed above, took longer than expected and unfortunately precluded obtaining more detailed information on important features of the ERPIC.

Are pre-existing peroxisomes the final site of the sorted myc*AtPEX16?*

The temporal fate of *myc*AtPEX16 within the ERPIC is an important consideration as evidenced by recent models that portray different fates within varied schemes for peroxisome biogenesis. For example, ER-derived membrane structures (carriers) bearing PMPs detach and form in the cytosol new mature peroxisomes within mammalian and yeast cells (Kunau, 2005; Kim *et al*., 2006; Titorenko and Mullen, 2006; van der Zand *et al*., 2006), whereas in plant cells such structures are predicted to fuse with pre-existing peroxisomes (Trelease and Lingard, 2006) that divide constitutively (via fission?) to form new peroxisomes that end up in daughter cells following cytokinesis (Lingard and Trelease, 2006).

The current results are most consistent with the *myc*AtPEX16 in ERPIC ending up within pre-existing peroxisomes. This contention is based primarily on the virtual 100% colocalizations, under normal and experimental conditions, of *myc*AtPEX16 with catalase (Figs 1, 3, 5) or APX (Fig. 2) in virtually every peroxisome observed in both cell types. If new peroxisomes were formed from maturation of ERPIC components, one should readily observe *myc*AtPEX16-bearing peroxisomes without catalase (or APX). If, however, forming new peroxisomes acquired catalase and APX from the cytosol, then one would clearly observe pre-existing catalase- or APX-bearing peroxisomes without *myc*-labelled AtPEX16. Alternatively, *myc*AtPEX16-bearing structures might do both, i.e. form new peroxisomes and fuse with pre-existing peroxisomes. In this case, all of the peroxisomes would bear *myc* fluorescence signals (as was observed), but the number of total peroxisomes per cell would be increased. Although this would be difficult to visualize or quantify in BY-2 cells (small, numerous peroxisomes), it would be readily observed in *Arabidopsis* suspension cells, even without quantification (examples in Lingard and Trelease, 2006). Thus we are confident from our multitude of microscopy observations that ER-derived *myc*AtPEX16 sorts to pre-existing plant peroxisomes, most likely via some sort of membrane carrier(s) within ERPIC.

Molecular targeting signals for trafficking AtPEX16 to pre-existing peroxisomes

Membrane peroxisome targeting signal(s) (mPTSs) can be defined experimentally as necessary and/or sufficient for trafficking the native protein, or a heterologous reporter protein, respectively, to one or more compartments within a particular sorting pathway (Heiland and Erdmann, 2005; Van Ael and Fransen, 2006). mPTSs are considered to consist of at least two functional domains, i.e. a membrane targeting element and a membrane anchoring domain. For example, the type 1 mPTS (mPTS1), characteristic of PMPs sorted directly to peroxisomes, is composed of a stretch, or non-adjacent cluster, of positively charged amino acid residues plus an adjacent (or nearby) transmembrane domain (membrane helix) (Dyer *et al*., 1996; Wang *et al*., 2001; Hunt and Trelease, 2004). The type 2 mPTS (mPTS2), predicted for AtPEX16, is composed of an mPTS1-like signal in addition to an 'ER targeting element', which may overlap or exist adjacent to the peroxisomal targeting element (Elgersma *et al*., 1997; Baerends *et al*., 2000; Mullen and Trelease, 2000).

As mentioned above, the human PEX16 has been described both as a Group I and a Group II PMP. Honsho *et al*. (2002), who considered HsPEX16 as a Group II PMP with two internal membrane helices, examined its direct targeting to the pre-existing peroxisomes in cultured Chinese hamster ovary cells. They concluded that an internal sequence of clustered basic amino acid residues (positions 61–81) plus its MH1 downstream of nearly 40 amino acids was both necessary and sufficient for direct targeting to the peroxisomes. Interestingly, in studies with the same PMP, Kim *et al*. (2006) found that delivery of HsPEX16 from the ER, where it was co-translationally inserted, to peroxisomes was dependent upon the same cluster of 16 basic amino acid residues, but not upon the downstream MH1. Notably however, their targeting construct (appended to GFP) possessed both MHs. In the current study, transport of GFP or the native AtPEX16 first to the ER and then peroxisomes was also dependent upon an internal cluster of basic amino acids. However, its topological position was distinct from the necessary cluster in HsPEX16; it was between the two MHs rather than substantially upstream from MH1. It was possible to discern in more detail that only the tripeptide -VRS- plus only one of the MHs (MH1) was essential for targeting indirectly to the plant peroxisomes. It is not clear why only one MH was not sufficient for trafficking AtPEX16 to the peroxisomes.

Of four different plant PMPs examined, namely GhAPX, AtPMP22, AtPEX3, and AtMDAR (Mullen and Trelease, 2000; Murphy *et al*., 2003; Hunt and Trelease, 2004; Lisenbee *et al*., 2005), only APX was found to possess an mPTS2 that targets the protein to peroxisomes indirectly via ER (Mullen and Trelease, 2000). The authors found that a patch of five basic residues (RKRMK) within the hydrophilic C-terminal-most amino acid residues was necessary but not sufficient for sorting. Instead, the basic residues plus the immediately adjacent TMD was sufficient for sorting. However, the signal guiding APX from the cytosol to ER and the one guiding APX from ER to peroxisomes overlapped and could not be distinguished. Similar to AtPEX16, the chimeric proteins or mutated constructs of APX either sorted to peroxisomes via ER or ended up in the cytosol (Table 2). In no case, did the constructs localize exclusively in ER and not sort to the peroxisomes. Hence, it can be concluded that, like APX, the necessary and sufficient ER and peroxisome targeting signals for AtPEX16 are overlapping.

In summary, this dynamic *in vivo* study on the indirect trafficking and signal-mediated sorting of transiently expressed AtPEX16 through ER to pre-existing peroxisomes, which was spawned from previous knowledge that endogenous AtPEX16 co-existed in non-transformed plant cells, constitutes the most comprehensive examination of a Group I PMP (peroxin or otherwise) relative to the biogenesis of plant peroxisomes. Data were obtained and the significance discussed for each subcellular site encountered along the entire pathway beginning with the appearance of the nascent protein in the cytosol and ending its signalled trek within the boundary membrane of peroxisomes already present in the cytoplasm. Documented participation of the reticular ER and the novel yet mostly undefined ERPIC (Titorenko and Mullen, 2006) is congruent with the most recent models for biogenesis of peroxisomes in other organisms (Kunau, 2005; Trelease and Lingard, 2006; van der Zand *et al*., 2006). However, it must be noted that the main role of the ER in most other organisms is in the formation of new peroxisomes, whereas its known role in plants is one of providing and delivering proteins and lipid within membrane carriers to peroxisomes for normal maintenance and/or maturation/differentiation of functional peroxisomes. Progeny peroxisomes in divided cells apparently are produced via binary fission of mature peroxisomes in response to direct or indirect induction of PEX11 isoforms (Lingard and Trelease, 2006), thus completing the cycle of peroxisome biogenesis in plants. A recent model portraying most of these aspects outlined above is described and referred to as the 'ER-semiautonomous peroxisomal growth and division' model (Trelease and Lingard, 2006). Considering the new data and interpretations present in the current paper, an appropriate updated version of this model, namely the 'ER semi-autonomous peroxisome maturation and replication' model, has been presented (Mullen and Trelease, 2006).

Acknowledgements

We thank all those who donated antibodies used in this study (listed in the Materials and methods). Dr Andreas Nebenführ and Dr Andrew Staehelin are thanked for providing the GmMan1::(GFP) plasmid used in this study. Heather Gustafson and Daisy Savarirajan maintained the *Arabidopsis* and BY-2 cell cultures. Special thanks are extended to Drs Scott Bingham, Matthew J. Lingard, Robert Mullen, and Cayle Lisenbee for their advice, insightful discussions, and encouragement on the various aspects of this research. This work was supported by the National Science Foundation (grant no. MCB-0091826) to RNT and in part by the William N. and Myriam Pennington Foundation. The graduate programme in Molecular and Cellular Biology at Arizona State University funded Research Assistantships to SKK.

References

Baerends R, Faber K, Kiel J, Van der Klei I, Harder W, Veenhuis M. 2000. Sorting and function of peroxisomal membrane proteins. *FEMS Microbiology Reviews* **24,** 291–301.

Baker A, Graham I, eds. 2002. *Plant peroxisomes. Biochemistry, cell biology and biotechnological applications*. Dordecht, Netherlands: Kluwer Academic Publishers.

Baker A, Sparkes I. 2005. Peroxisome protein import: some answers, more questions. *Current Opinion in Plant Biology* **8,** 640–647.

Brocard C, Boucher K, Jedeszko C, Kim P, Walter P. 2005. Requirement for microtubules and dynein motors in the earliest stages of peroxisome biogenesis. *Traffic* **6,** 1–10.

Bunkelmann J, Trelease R. 1996. Ascorbate peroxidase: a prominent membrane protein in oil seed glyoxysomes. *Plant Physiology* **110,** 589–598.

Corpas F, Bunkelmann J, Trelease R. 1994. Identification and immunochemical characterization of a family of peroxisome membrane-proteins (Pmps) in oilseed glyoxysomes. *European Journal of Cell Biology* **65,** 280–290.

Corpas F, Trelease R. 1998. Differential expression of ascorbate peroxidase and a putative molecular chaperone in the boundary membrane of differentiating cucumber seedling peroxisomes. *Journal of Plant Physiology* **153,** 332–338.

Coughlan S, Hastings C, Winfrey R. 1997. Cloning and characterization of the calreticulin gene from *Ricinus communis* L. *Plant Molecular Biology* **34,** 897–911.

del Rio L, Corpas F, Sandalio L, Palma J, Gomez M, Barroso J. 2002. Reactive oxygen species, antioxidant systems and nitric oxide in peroxisomes. *Journal of Experimental Botany* **53,** 1255–1272.

del Rio L, Sandalio L, Corpas F, Palma J, Gomez M, Barroso J. 2006. Reactive oxygen species and reactive nitrogen species in peroxisomes: production, scavenging, and role in cell signaling. *Plant Physiology* **141,** 330–335.

Distel B, Erdmann R, Gould S, *et al*. 1996. A unified nomenclature for peroxisome biogenesis factors. *Journal of Cell Biology* **135,** 1–3.

Dyer J, McNew J, Goodman J. 1996. The sorting sequence of the peroxisomal integral membrane protein PMP47 is contained within a short hydrophilic loop. *Journal of Cell Biology* **133,** 269–280.

Eckert J, Erdmann R. 2003. Peroxisome biogenesis. *Reviews of Physiological Biochemical Pharmacology* **147,** 75–121.

Elgersma Y, Kwast L, van den Berg M, Snyder W, Distel B, Subramani S, Tabak H. 1997. Overexpression of Pex15p, a phosphorylated peroxisomal integral membrane protein required for peroxisome assembly in *S. cerevisiae*, causes proliferation of the endoplasmic reticulum membrane. *EMBO Journal* **16,** 7326–7341.

Erdmann R, Schliebs W. 2005. Peroxisomal matrix protein import: the transient pore model. *Nature Reviews Molecular Cell Biology* **6,** 738–742.

Flynn C, Heinze M, Schumann U, Gietl C, Trelease R. 2005. Compartmentalization of the plant peroxin, AtPex10p, within subdomain(s) of ER. *Plant Science* **168,** 635–652.

Geuze H, Murk J, Stroobants A, Griffith J, Kleijmeer M, Koster A, Verkleij A, Distel B, Tabak H. 2003. Involvement of the endoplasmic reticulum in peroxisome formation. *Molecular Biology of the Cell* **14,** 2900–2907.

Guo T, Kit Y, Nicaud J, Le Dall M, Sears S, Vali H, Cahn H, Rachubinski R, Titorenko V. 2003. Peroxisome division in the yeast *Yarrowia lipolytica* is regulated by a signal from inside the peroxisome. *Journal of Cell Biology* **162,** 1255–1266.

Haan G, Baerends R, Krikken A, Otzen M, Veenhuis M, van der Klei I. 2006. Reassembly of peroxisomes in *Hansenula polymorpha* pex3 cells on reintroduction of Pex3p involves the nuclear envelope. *FEMS Yeast Research* **6,** 186–194.

Hawes C. 2005. Cell biology of the plant Golgi apparatus. *New Phytologist* **165,** 29–44.

Heiland I, Erdmann R. 2005. Biogenesis of peroxisomes topogenesis of the peroxisomal membrane and matrix proteins. *FEBS Journal* **272,** 2362–2372.

Hobman T, Zhao B, Chan H, Farquhar M. 1998. Immunoisolation and characterization of a subdomain of the endoplasmic reticulum that concentrates proteins involved in COPII vesicle biogenesis. *Molecular Biology of the Cell* **9,** 1265–1278.

Hoepfner D, Schildknegt D, Braakman I, Philippsen P, Tabak H. 2005. Contribution of endoplasmic reticulum to peroxisome formation. *Cell* **122,** 85–95.

Honsho M, Hiroshige T, Fujiki Y. 2002. The membrane biogenesis peroxin Pex16p: topogenesis and functional roles in peroxisomal membrane assembly. *Journal of Biological Chemistry* **277,** 44513–44524.

Hunt J, Trelease R. 2004. Sorting pathway and molecular targeting signals for the Arabidopsis peroxin 3. *Biochemical and Biophysical Research Communications* **314,** 586–596.

Karnik SK, Trelease RN. 2005. Arabidopsis peroxin 16 coexists at steady state in peroxisomes and endoplasmic reticulum. *Plant Physiology* **138,** 1967–1981.

Kim P, Mullen R, Schumann U, Lipincott-Schwartz J. 2006. The origin and maintenance of mammalian peroxisomes involves a *de novo* PEX16-dependent pathway from the ER. *Journal of Cell Biology* **173,** 521–532.

Kragt A, Voom-Brouwer T, van der Berg M, Distel B. 2005. Endoplasmic reticulum-directed Pex3p routes to peroxisomes and restores peroxisome formation in *Saccharomyces cerevisiae* pex3Delta strain. *Journal of Biological Chemistry* **280,** 34350–34357.

Kunau W. 2005. Peroxisome biogenesis: end of debate. *Current Biology* **15,** 774–776.

Kunce C, Trelease R, Turley R. 1988. Purification and biosynthesis of cottonseed (*Gossypium hirsutum* L.) catalase. *Biochemical Journal* **251,** 147–155.

Lazarow P. 2003. Peroxisome biogenesis: advances and conundrums. *Current Opinion in Cell Biology* **15,** 489–497.

Lazarow P, Fujiki Y. 1985. Biogenesis of peroxisomes. *Annual Review of Cell Biology* **1,** 489–530.

Lee M, Mullen R, Trelease R. 1997. Oilseed isocitrate lyases lacking their essential type I peroxisomal targeting signal are piggybacked to glyoxysomes. *The Plant Cell* **9,** 185–197.

Lin Y, Cluette-Brown J, Goodman H. 2004. The peroxisome deficient *Arabidopsis* mutant *sse1* exhibits impaired fatty acid synthesis. *Plant Physiology* **135,** 814–827.

Lin Y, Sun L, Nguyen L, Rachubinski R, Goodman H. 1999. The pex16p homolog SSE1 and storage organelle formation in Arabidopsis seeds. *Science* **284,** 328–330.

Lingard M, Trelease R. 2006. Five *Arabidopsis* homologs individually promote peroxisome elongation, duplication or aggregation. *Journal of Cell Science* **119,** 1961–1972.

Lisenbee C, Lingard M, Trelease R. 2005. Arabidopsis peroxisomes possess functionally redundant membrane and matrix isoforms of monodehydroascorbate reductase. *The Plant Journal* **43,** 900–914.

Lisenbee C, Heinze M, Trelease R. 2003*a*. Peroxisomal ascorbate peroxidase resides within a subdomain of rough endoplasmic reticulum in wild-type Arabidopsis cells. *Plant Physiology* **132,** 870–882.

Lisenbee C, Karnik S, Trelease R. 2003*b*. Overexpression and mislocation of a tail-anchored GFP redefines the identity of peroxisomal ER. *Traffic* **4,** 491–501.

Martinez-Alonso E, Gustavo E, Ballesta J, Martinez-Menarguez J. 2005. Structure and dynamics of the Golgi complex at 15 °C: low temperature induces the formation of Golgi-derived tubules. *Traffic* **6,** 32–44.

McCartney A, Greenwood J, Fabian M, White K, Mullen R. 2005. Localization of the tomato bushy stunt virus replication protein p33 reveals a peroxisome-to-endoplasmic reticulum sorting pathway. *The Plant Cell* **17,** 3513–3531.

Movafeghi A, Happel N, Pimpl P, Tai G, Robinson D. 1999. Arabidopsis Sec21p and Sec23p homologs: probable coat proteins of plant cop-coated vesicles. *Plant Physiology* **19,** 1437–1445.

Mullen R, Flynn C, Trelease R. 2001*a*. How are peroxisomes formed? The role of the endoplasmic reticulum and peroxins. *Trends in Plant Science* **6,** 256–261.

Mullen R, Lisenbee C, Flynn C, Trelease R. 2001*b*. Stable and transient expression of chimeric peroxisomal membrane proteins induces an independent 'zippering' of peroxisomes and an endoplasmic reticulum subdomain. *Planta* **213,** 849–863.

Mullen R, Lisenbee C, Miernyk J, Trelease R. 1999. Peroxisomal membrane ascorbate peroxidase is sorted to a membranous network that resembles a subdomain of the endoplasmic reticulum. *The Plant Cell* **11,** 2167–2185.

Mullen R, Trelease R. 2000. The sorting signals for peroxisomal membrane-bound ascorbate peroxidase are within its C-terminal tail. *Journal of Biological Chemistry* **275,** 16337–16344.

Mullen R, Trelease R. 2006. The ER-peroxisome connection in plants: development of the 'ER semi-autonomous peroxisome maturation and replication' model for plant peroxisome biogenesis. *Biochimica et Biophysica Acta–Molecular Cell Research* **1763,** 1655–1668.

Murphy M, Phillipson B, Baker A, Mullet R. 2003. Characterization of the targeting signal of the Arabidopsis 22-kD integral peroxisomal membrane protein. *Plant Physiology* **133,** 813–828.

Nebenführ A. 2002. Vesicle traffic in the endomembrane system: a tale of COPs, Rabs and SNARES. *Current Opinion in Plant Biology* **5,** 507–512.

Nebenführ A, Gallagher L, Dunahay T, Frohlick J, Mazurkiewiez A, Meehl J, Staehelin L. 1999. Stop-and-go movements of plant Golgi stacks are mediated by the acto-myosin system. *Plant Physiology* **121,** 1127–1142.

Pimpl P, Movafeghi A, Coughlan S, Denecke J, Hillmer S, Robinson D. 2000. *In situ* localization and *in vitro* induction of plant COPI-coated vesicles. *The Plant Cell* **12,** 2219–2236.

Purdue P, Lazarow P. 2001. Peroxisome biogenesis. *Annual Reviews in Cell and Developmental Biology* **17,** 701–752.

Ritzenthaler C, Nebenführ A, Movafeghi A, Stussi-Garaud C, Behnia L, Pimpl P, Staehelin L, Robinson D. 2002. Reevaluation of the effects of brefeldin A on plant cells using tobacco bright yellow 2 cells expressing Golgi-targeted green fluorescent protein and COPI antisera. *The Plant Cell* **14,** 237–261.

Saraste J, Kuismanen E. 1984. Pre- and post-Golgi vacuoles operate in the transport of Semiliki forest virus membrane glycoproteins to the cell surface. *Cell* **38,** 535–549.

Schumann U, Wanner G, Veenhuis M, Schmid M, Gietl C. 2003. AthPEX10, a nuclear gene essential for peroxisome and storage organelle formation during Arabidopsis embryogenesis. *Proceedings of the National Academy of Sciences, USA* **100,** 9626–9631.

South S, Gould S. 1999. Peroxisome synthesis in the absence of preexisting peroxisomes. *Journal of Cell Biology* **144,** 255–266.

Sparkes I, Baker A. 2002. Peroxisomes biogenesis and protein import in plants, animals and yeasts: enigma and variations? *Molecular Membrane Biology* **19,** 171–185.

Sparkes I, Hawes C, Baker A. 2005. AtPEX2 and AtPEX10 are targeted to peroxisomes independently of known endoplasmic reticulum trafficking routes. *Plant Physiology* **193,** 690–700.

Tam Y, Fagarasanu A, Fagarasanu M, Rachubinski R. 2005. Pex3p initiates the formation of a preperoxisomal compartment from a subdomain of the endoplasmic reticulum in *Saccharomyces cerevisiae*. *Journal of Biological Chemistry* **280,** 34933–34939.

Titorenko V, Mullen R. 2006. 'Peroxisome biogenesis': the peroxisomal endomembrane system and the role of the ER. *Journal of Cell Biology* **174,** 11–17.

Titorenko V, Rachubinski R. 1998. Mutants of the yeast *Yarrowia lipolytica* defective in protein exit from the endoplasmic reticulum are also defective in peroxisome biogenesis. *Molecular Cell Biology* **18,** 2789–2803.

Titorenko V, Rachubinski R. 2000. Peroxisomal membrane fusion requires two AAA family ATPases Pex1p and Pex6p. *Journal of Cell Biology* **150,** 881–886.

Titorenko V, Rachubinski R. 2001*a*. Dynamics of peroxisome assembly and function. *Trends in Cell Biology* **11,** 22–29.

Titorenko V, Rachubinski R. 2001*b*. The life cycle of the peroxisome. *Nature Reviews in Molecular and Cell Biology* **2,** 357–368.

Trelease R, Lingard M. 2006. Participation of the plant ER in peroxisomal biogenesis. In: Robinson DG, ed. *The plant endoplasmic reticulum*. Plant Cell Monographs No. 4. Heidelberg: Springer-Verlag, 205–232.

Trelease R. 2002. Peroxisomal biogenesis and acquisition of membrane proteins. In: Baker A, Graham I, eds. *Plant peroxisomes*. Dordrecht: Kluwer Academic Publishers, 305–337.

Van Ael E, Fransen M. 2006. Targeting signals in peroxisomal membranes. *Biochimica et Biophysica Acta–Molecular Cell Research* 10.1016/j.bbamer.2006.08.020.

van der Zand A, Braakman I, Geuze H, Tabak H. 2006. The return of the peroxisome. *Journal of Cell Science* **119,** 989–994.

Wang X, Unruh M, Goodman J. 2001. Discrete targeting signals direct PMP47 to oleate-induced peroxisomes in *Saccharomyces cerevisiae*. *Journal of Biological Chemistry* **276,** 10897–10905.

Yang Y, Elamawi R, Bubeck J, Pepperkok R, Ritzenthaler C, Robinson D. 2005. Dynamics of COPII vesicles and the Golgi apparatus in cultured *Nicotiana tabacum* BY-2 cells provides evidence for transient association of Golgi stacks with endoplasmic reticulum exit sites. *The Plant Cell* **17,** 1513–1531.

Zacharias D, Violin J, Newton A, Tsien R. 2002. Partioning of lipid-modified monomeric GFPs into membrane microdomains of live cells. *Science* **296,** 913–916.